The Phase Behavior and Organization of Sphingomyelin/Cholesterol Membranes: A Deuterium NMR Study

Amir Keyvanloo,[1] Mehran Shaghaghi,[1] Martin J. Zuckermann,[1] and Jenifer L. Thewalt[1,2,*]

[1]Department of Physics and [2]Department of Molecular Biology and Biochemistry, Simon Fraser University, Burnaby, British Columbia, Canada

ABSTRACT We have studied the dependence of the phase and domain characteristics of sphingomyelin (SM)/cholesterol model membranes on sterol content and temperature using deuterium nuclear magnetic resonance. NMR spectra of N-palmitoyl(D31)-D-erythro-sphingosylphosphorylcholine (PSM-d31) were taken for temperatures from 25 to 70°C and cholesterol concentrations of 0–40%. Analogous experiments were performed using 1-palmitoyl,2-palmitoyl(D31)-*sn*-glycero-3-phosphocholine (DPPC-d31)/cholesterol membranes to carefully compare the data obtained using palmitoyl chains that have similar "kinked" conformations. The constructed phase diagrams exhibit both solid-ordered (so) + liquid-ordered (lo) and liquid-disordered (ld) + lo phase-coexistence regions with a clear three-phase line. Macroscopic (micron-sized) coexistence of ld and lo phases was not observed; instead, line-broadening in the ld+lo region was characterized by intermediate exchange of lipids between the two types of domains. The length scales associated with the domains were estimated to be 75–150 nm for PSM-d31/cholesterol and DPPC-d31/cholesterol model membranes.

INTRODUCTION

Lipid-lipid interactions are important determinants of membrane organization in living systems and have been thoroughly researched for a variety of membranes (1–6). The lipid composition of the outer leaflet of a typical mammalian plasma membrane is mainly sphingomyelin (SM), cholesterol, and unsaturated phosphatidylcholine (PC) (7,8). The preferential association of SM and cholesterol has been observed in a wide variety of membrane environments. For example, detergent-resistant membranes are rich in SM/cholesterol (9), and SM and cholesterol are associated in distinct ordered phases in three-component giant unilamellar vesicles (GUVs) (10,11). In addition, such an association has been found in small domains directly observed in membranes of living cells (12–17).

Despite the intense research into the nature of lipid-cholesterol interactions, there remain several outstanding questions concerning the role of cholesterol and other sterols in forming the tightly-packed liquid-ordered (lo) phase. For example, liquid-disordered (ld) and lo phases were found to coexist in dipalmitoyl PC (DPPC)/sterol

model membranes (18–20), but the two phases were not observed to coarsen, remaining sub-microscopic in size. Since their small size renders these dynamic domains invisible by most imaging techniques, and since an explanation for the lack of coarsening remains elusive, it has been postulated that there is no ld/lo phase coexistence in DPPC/cholesterol model membranes. An alternative explanation for such membrane heterogeneity invokes lipid-composition fluctuations due to proximity to a critical point (21). Theoretical descriptions of phospholipid-sterol interactions are numerous (22–26), and the area continues to be very active as simulation strategies improve and accurate experimental input parameters become available (27). The original PC/sterol "complex" model (28) has been modified to predict phase coexistence in DPPC/cholesterol model membranes above the main transition temperature (29).

Many investigations into membrane phase behavior have attempted to reproduce the important aspects of outer-leaflet organization by combining a "low-melting" lipid, often dioleoyl PC (DOPC), and a high-melting lipid, often DPPC, with cholesterol. Such membranes are not "natural," as neither DOPC nor DPPC is found in most biological membranes, but their study has provided considerable insight into fundamental lipid physical chemistry, and particularly

into the lo+ld phase coexistence region of the ternary phase diagram. Furthermore, DPPC has been postulated to be a reasonable analog for SM in such studies, since palmitoylsphingomyelin (PSM) and DPPC have similar chain-melting transition temperatures and chain lengths and identical phosphocholine headgroups. Sphingomyelin-containing lipid membranes have also been studied in some detail (see reviews (30,31)). The combination of POPC, PSM, and cholesterol is particularly attractive, since all three lipids are found in nature and together make an excellent model for the mammalian plasma membrane outer leaflet. Large-scale lo+ld phase coexistence was observed for some regions of the phase diagram (10,11) of this system, and an lo phase was found at sufficiently high cholesterol concentrations (2,32,33).

Despite this ongoing progress with the three-component system, there is still much to learn about the phase behavior and physical properties of binary sphingolipid/sterol membranes. Several groups have published results indicating that ld+lo phase coexistence occurs in SM/cholesterol (11,30,32,34,35), providing insight into, and partial determinations of, the binary phase diagram. A comparison of the investigations of these groups into the properties of SM/cholesterol model membranes is, however, complicated by the fact that SM from different sources differs in the chemical mixture of its constituent chains. To directly assess the nature of the interaction between sphingomyelin and cholesterol, we have performed a detailed phase-diagram determination of this system using deuterium nuclear magnetic resonance (^{2}H NMR) and pure palmitoyl chain perdeuterated PSM (PSM-d31). Since the N-linked palmitoyl chain of PSM is structurally analogous to the *sn*-2 chain of DPPC, we chose to re-determine the DPPC/cholesterol phase diagram (18) using *sn*-2-chain-perdeuterated DPPC (DPPC-d31). In this way, we can directly compare and contrast the effect of cholesterol on the phase behavior and chain order of these two lipids.

MATERIALS AND METHODS

Sample preparation

DPPC-d31 (*sn-2* chain perdeuterated) and PSM-d31 were obtained from Avanti Polar Lipids (Alabaster, AL). Cholesterol and deuterium-depleted water were obtained from Sigma-Aldrich Canada (Oakville, Ontario, Canada). Lipid/cholesterol multilamellar dispersions (MLDs) were prepared by adding cholesterol concentrations of 0, 2.6, 5, 8, 10.1, 12, 16, 18, 20.5, 25, 29.9, 40, and 45 mol % to DPPC-d31 and concentrations of 0, 2.5, 5.4, 8.5, 11, 14.5, 17.5, 20, 22.5, 25, 28, 31.5, 35, and 40 mol % to PSM-d31. Each DPPC-d31/cholesterol sample was made separately using ~50 mg lipid. Lipid and cholesterol were mixed and dissolved in Bz/MeOH 4:1 (v/v) and then freeze-dried. PSM-d31/cholesterol samples were made by gradually adding cholesterol to PSM-d31, starting from 50 mg sphingomyelin. Each PSM-d31/cholesterol sample was lyophilized after being recovered from the NMR tube and it was then dissolved in Bz/MeOH 4:1 (v/v) and freeze-dried again to remove residual water. In the next step, an appropriate amount of cholesterol was added (from the Bz/MeOH stock solution) to the sample and then freeze-dried. All samples were hydrated using deuterium-depleted water to form MLDs. Hydration was performed by freeze-thaw-vortex cycling five times between liquid nitrogen temperature and 60°C.

^{1}H solution NMR (at 300 K) in MeOH-d$_4$ was used to test cholesterol concentration by integrating non-composite peaks arising from the two components. Specifically, these were the methyl peak at 0.74 ppm and the H-6 peak at 5.36 ppm for cholesterol; the glycerol-c2 peak at 5.26 ppm and the γ-(CH$_3$)$_3$ peak at 3.24 ppm for DPPC; and the sphingosine C2 proton resonance at 5.47 ppm and the γ-(CH$_3$)$_3$ peak at 3.24 ppm for sphingomyelin. All chemical shifts were measured with respect to the MeOH-d$_4$ methyl peak at 3.32 ppm (with assignments of cholesterol and DPPC peaks taken from Muhr et al. (36) and Peng et al. (37), respectively). After completion of the NMR experiments, several samples were checked for degradation by thin-layer chromatography (TLC), eluting with CHCl$_3$/MeOH/H$_2$O 65:25:4 v/v. These include every other sample in the case of PSM-d31/cholesterol, and every third sample in the case of DPPC-d31/cholesterol. The ^{2}H NMR experiments took 3–4 days per DPPC-d31/cholesterol sample and 4–10 days for PSM-d31/cholesterol samples, but no degradation of any of the samples could be detected by TLC. Also, no sign of degradation was evident in the ^{1}H NMR spectra.

^{2}H NMR spectroscopy

^{2}H NMR experiments were performed on a locally built spectrometer at 46.8 MHz using the quadrupolar echo technique (38). The typical spectrum resulted from 10,000 to 40,000 repetitions of the two-pulse sequence with 90° pulse lengths of 3.95 μs, interpulse spacing of 40 μs, and dwell time of 2 μs. The delay between acquisitions was 300 ms, and data were collected in quadrature with Cyclops eight-cycle phase cycling. The fluid-phase spectra were dePaked using an iterative method (39). However, some dePaked spectra exhibited unphysical negative amplitudes, indicating that liposomes are partially oriented in the magnetic field. In these cases, the regularization dePakeing algorithm was used (40). Smoothed order parameter profiles were extracted from the dePaked spectra using an established procedure (41). The spin-spin relaxation time, T_{2e}, was measured by varying the interpulse spacing from 40 to 100 μs and taking the initial slope of the echo peak signal versus echo time. Values of T_{2e} were used to correct the so+lo region of the phase diagram (see Supporting Material). The samples were heated from 25 to 70°C. At each temperature, the sample was allowed to equilibrate for 20 min before a measurement was taken.

The first moment, or average spectral width, M_1, was calculated using

$$M_1 = \frac{1}{2A} \sum_{\omega=-x}^{x} |\omega| f(\omega), \tag{1}$$

where ω is the frequency shift from the Larmor frequency, x was chosen so that the frequency range $-x$ to x contains the entire spectrum, $f(\omega)$ is the spectral intensity, and $A = \sum_{\omega=-x}^{x} f(\omega)$.

The order parameter $S_{CD} = \langle 3 \cos^2 \theta - 1 \rangle / 2$ was calculated from

$$\Delta \nu_Q = \frac{3}{4} (167 \text{ kHz}) |S_{CD}|, \tag{2}$$

where θ is the angle between the carbon-deuteron vector and the bilayer normal, $\Delta \nu_Q$ is the quadrupolar splitting of the deuterons on the local carbon, measured from the powder pattern, and 167 kHz is the static quadrupolar coupling constant.

Within the so+lo phase-coexistence region, a ^{2}H NMR spectrum consists of different amounts of endpoint spectra characteristic of the two phases in equilibrium, and the phase boundaries (x_s and x_f) are determined by the spectral subtraction method (see (18) and Supporting Material for more details).

RESULTS AND DISCUSSION

Distinct phases are observed

Depending on temperature and composition, both PSM-d31/cholesterol and DPPC-d31/cholesterol MLDs can exist in three distinct phases: the gel or solid-ordered (so) phase, the L_α or liquid-disordered (ld) phase, and the liquid-ordered (lo) phase. The ^{2}H NMR spectra of these phases have unique characteristics that can be used to map phase boundaries and regions of phase coexistence. Fig. 1 shows the spectra representative of these three phases for PSM-d31/cholesterol and DPPC-d31/cholesterol MLDs, respectively.

The spectra in Fig. 1, A and A' are typical of the membrane ld phase. The ld spectrum is a superposition of Pake doublets; each doublet corresponds to a labeled carbon along the chain and is itself a powder pattern with a quadrupolar splitting representative of the local carbon-deuterium bond order parameter, S_{CD}. In this phase, the lipid chains have a relatively high population of *gauche* conformers and *gauche-trans* isomerization is very rapid. The lipid molecules undergo rapid axially symmetric reorientation about the bilayer normal (42,43) and are loosely packed laterally within the bilayer, leading to rapid lateral diffusion (34).

Fig. 1, B and B' show the spectra representative of the lo phase. The lo phase spectrum has a line shape qualitatively similar to that of the ld phase: the spectrum is again a superposition of Pake doublets, indicating that the acyl chains undergo rapid axially symmetric reorientation about the bilayer normal (44,45). However, the average width of the lo phase spectrum is much larger than that of the ld phase spectrum, nearly 1.7 times larger for PSM-d31 and 1.9 times larger for DPPC-d31. This means that the quadrupolar splitting for each position on the chain is considerably larger in the lo phase than in the ld phase, and the lipid chains are
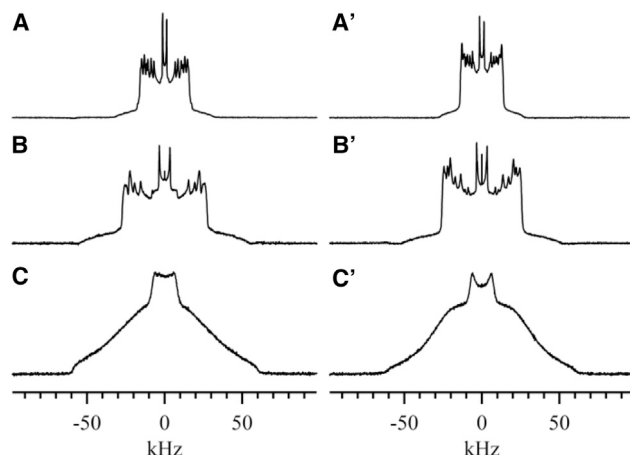
therefore highly conformationally ordered, with a reduced population of *gauche* conformers. Furthermore, the hydrocarbon chains approach the all-*trans* conformation at low temperatures (18), implying that the chain packing is much tighter in the lo phase than in the ld phase and that the rate of lateral diffusion is significantly reduced (34).

Fig. 1, C and C', show spectra characteristic of pure so-phase MLDs. Such spectra show that acyl chain deuterons in so-phase MLDs do not undergo rapid axially symmetric motion on the NMR timescale, since the lipids are closely packed. The significantly slower motions in the so phase lead to the characteristic bell-shaped spectrum of this phase (46,47).

Phase transitions

Since labeled lipids in each phase state possess a distinct ^{2}H NMR spectrum we can use the average spectral width, M_1, to characterize lipid phase behavior; phase changes can be detected by examining the spectra or M_1 as a function of temperature or composition. For instance, a large variation in M_1 with temperature can be used to pinpoint phase-transition temperatures in the membrane. Fig. 2, A and B, shows M_1 as a function of temperature for all PSM-d31/cholesterol and DPPC-d31/cholesterol MLDs, respectively. The gel (so) phase of pure DPPC-d31 MLDs exhibits a pretransition from the $L_{\beta'}$ phase to the $P_{\beta'}$ (ripple) phase near 32°C. Fig. 2 shows that in the absence of cholesterol, pure PSM-d31 and DPPC-d31 MLDs undergo main phase transitions (from the so phase to the ld phase) near $T_m = 40$°C. Adding cholesterol modifies both the ld and so phases of the lipid membranes. The $M_1(T)$ curve decreases less dramatically at T_m as more cholesterol is added; below T_m, M_1 decreases with increasing cholesterol concentration, whereas above T_m, it increases with increasing cholesterol concentration. Since M_1 is proportional to the average order parameter in the ld and/or lo phases, this shows that adding cholesterol increases the phospholipid's chain ordering above T_m.

Phase boundaries at low cholesterol content: so/(so + ld)/ld

The spectra shown in Fig. 3 A also illustrate the sharp main transition of pure PSM-d31 MLDs near 40°C. The spectra obtained below 39°C are characteristic of an so-phase membrane and those obtained above 41°C represent the ld phases. The spectrum collected at 40°C is composed of both so and ld components. The so component in such a so+ld spectrum is evident in the "shoulders" of the spectrum; so and ld spectral shoulders extend to $\sim \pm 60$ kHz and $\sim \pm 30$ kHz, respectively (Fig. 3 A). Therefore, the signal between 30 and 60 kHz (or between −30 and −60 kHz) is an indication of the so component. Spectra obtained above 41°C show only noise in this region, and thus, they contain no so component. Fig. 3 B displays the temperature dependence of spectra for the 94.6:5.4 PSM-d31/cholesterol
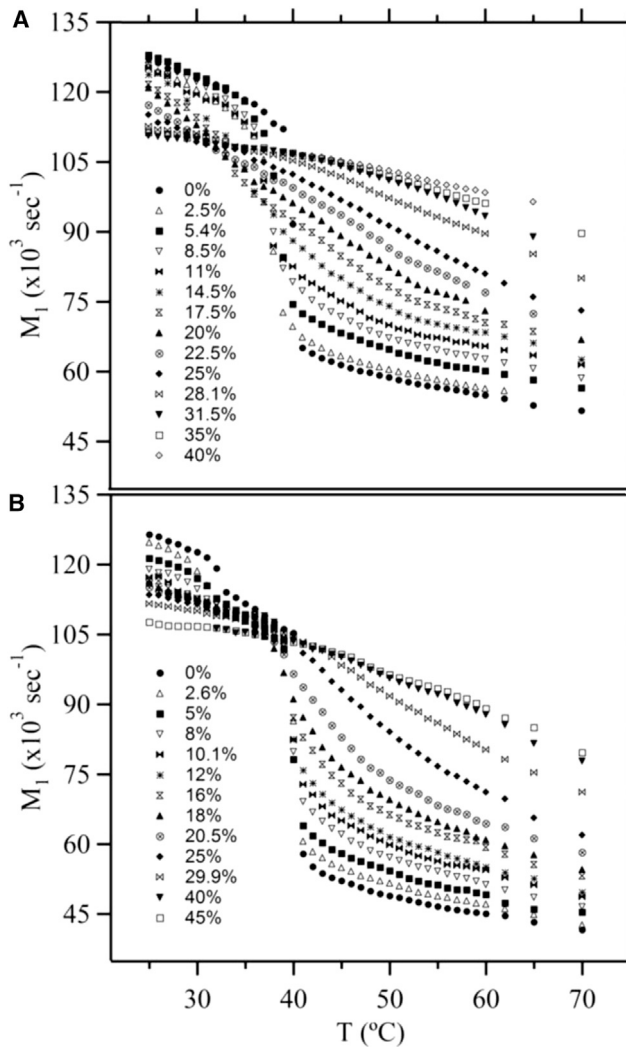

FIGURE 1 ^{2}H NMR spectra representative of three phases of PSM-d31 and DPPC-d31 membranes, respectively: (A and A') typical ld phases above 41°C. (B and B') lo phases with 40 mol % cholesterol at 48°C. (C and C') so phases below 39°C.

FIGURE 2 The temperature dependence of M_1 for (A) PSM-d31/cholesterol and (B) DPPC-d31/cholesterol at various cholesterol concentrations.

FIGURE 3 ^{2}H NMR spectra of (A) pure PSM-d31 and (B) 94.6:5.4 PSM-d31/cholesterol as a function of temperature.

MLDs. The spectrum obtained at 37°C displays both so and ld components, but with the so component dominating. The emergence of the 90° edges near ± 19 kHz confirms the existence of the ld component (the onset of the transition). The 39°C spectrum also contains both so and ld components, but the ld component dominates (the end of the transition). The trace of a residual so component in the tail of the spectrum is also visible, illustrated by the arrow in Fig. 3 B. Thus, the addition of 5.4 mol % cholesterol broadens the region of so and ld coexistence in PSM-d31 MLDs. This is true even for 2.5 mol % cholesterol, as shown by the more gradual slope of M_1 versus temperature (Fig. 2 A).

Phase boundaries at higher cholesterol content and low temperature: so/(so + lo)/lo

Fig. 4 shows the spectrum of PSM-d31/cholesterol MLDs as a function of cholesterol concentration at 31°C (i.e., below
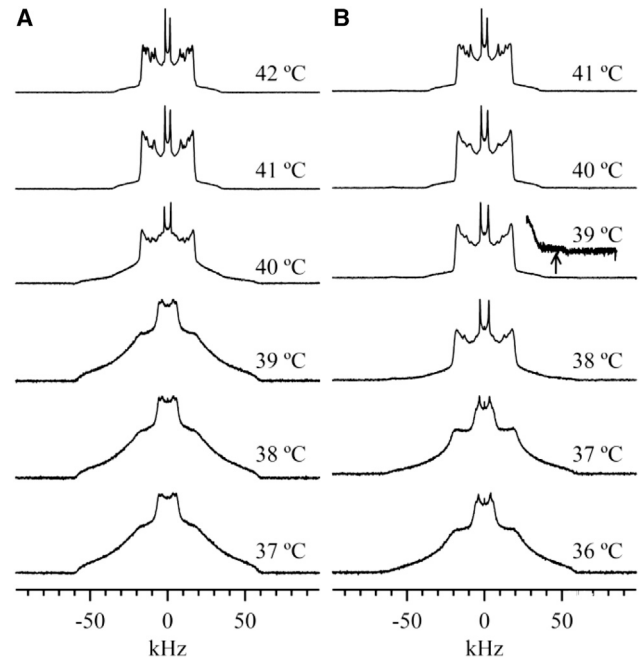
the T_m). Up to 8.5 mol % cholesterol, these MLDs display so-phase spectra. For the 11 mol % cholesterol sample, a small lo component appears in the so spectrum. This residual lo component can be detected by the emergence of peaks near ± 19 and ± 23 kHz. These peaks are more obvious in the 14.5 mol % sample. The coexistence of so and lo phases indicates that cholesterol induces lo domains in PSM-d31 MLDs. Fig. 4 shows that the fraction of lo phase increases as the concentration is increased within the two-phase region. Thermodynamically, this process corresponds to the growth of lo-phase domains at the expense of so-phase domains. In the presence of 25 mol % cholesterol, PSM-d31 MLDs appear to display a lo spectrum. However, it is not clear whether the so component has totally disappeared from this spectrum. Examining the shoulders of the spectrum as we did for the so+ld spectrum is difficult in this case, as the shoulders of so and lo spectra both extend to $\sim \pm 60$ kHz (see Fig. 1). When the cholesterol concentration reaches 31.5 mol % and higher, the spectra are consistent with lo-phase PSM-d31 MLDs. Therefore, the data of Fig. 4 imply a so/(so+lo) phase change occurring between 8.5 and 14.5 mol % and a (so+lo)/lo phase change between 22.5 and 28 mol % cholesterol. Further analysis is required to measure these phase boundaries accurately.

The ^{2}H NMR spectrum of PSM-d31/cholesterol MLDs within the two-phase region will be a superposition of its distinguishable components, provided that the domains are sufficiently large and exchange of the lipid molecules between the two domains is slow on the NMR timescale. In this case, spectral subtraction can be used to determine the
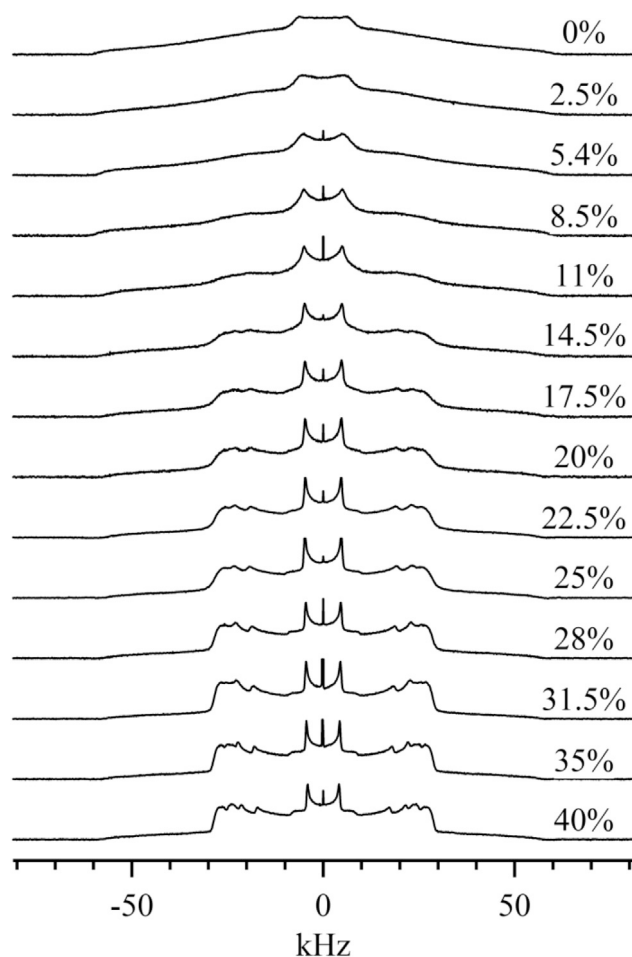
FIGURE 4 ^{2}H NMR spectra of PSM-d31/cholesterol as a function of cholesterol concentration at $T = 31°C$.

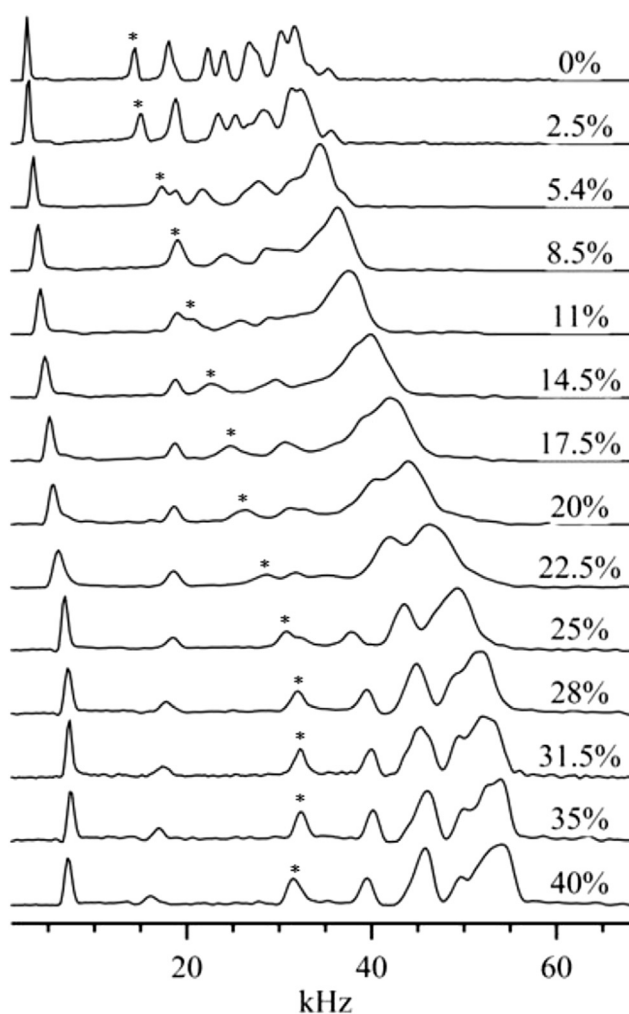
FIGURE 5 Half of the dePaked spectrum, at 47°C, of PSM-d31/cholesterol MLDs as a function of cholesterol concentration. The C15 peak, used in exchange-rate calculations, is labeled with an asterisk.

end-point spectra associated with phase boundaries (see the Supporting Material for details).

Phase boundaries at higher cholesterol content and high temperature: ld/(ld+lo)/lo

Adding cholesterol induces lo-phase domains in PSM-d31 MLDs. This can be qualitatively observed by examining the dePaked spectra of PSM-d31/cholesterol MLDs at a temperature above the T_m as a function of cholesterol concentration (see Fig. 5). For all temperatures below 55°C, the ld/ld+lo phase boundary was determined by direct examination of the dePaked spectra. For example, at 47°C (Fig. 5), the spectra exhibit the well-resolved "sharp" peaks associated with ld-phase membranes up to 8.5 mol % cholesterol. The width of the spectrum increases rapidly from 11 to 28 mol % cholesterol, and the spectra are blurry. We interpret this line-broadening in terms of lipid diffusion between the ld and lo domains at a rate faster than the NMR timescale. This implies that PSM-d31/cholesterol bilayers are in a heterogeneous state: ld and lo domains coexist.

A similar type of line broadening is apparent in oriented PSM-d31/cholesterol bilayers at 15 and 20 mol % cholesterol (32). The individual peaks become sharp again for cholesterol concentrations of 31.5 mol % and above. These spectra are representative of the lo phase, having quadrupolar splittings significantly larger than those of ld-phase spectra. Thus, the ld/ld+lo phase boundary lies between 8.5 and 11 mol % cholesterol, as indicated on the phase diagram (Fig. 7) and the ld+lo/lo phase boundary lies between 28 and 31.5 mol % cholesterol.

Further analysis allowed us to pinpoint the boundary between the ld+lo domain coexistence region and the lo phase. Fig. 6 shows the progression of the average order parameter, M_1, with increasing cholesterol concentration for several temperatures above the T_m. The average order parameter of MLDs containing coexisting lo and ld domains is expected to be particularly sensitive to increasing cholesterol concentration, because a portion of the ld phase will be converted to the more ordered lo phase upon the addition of
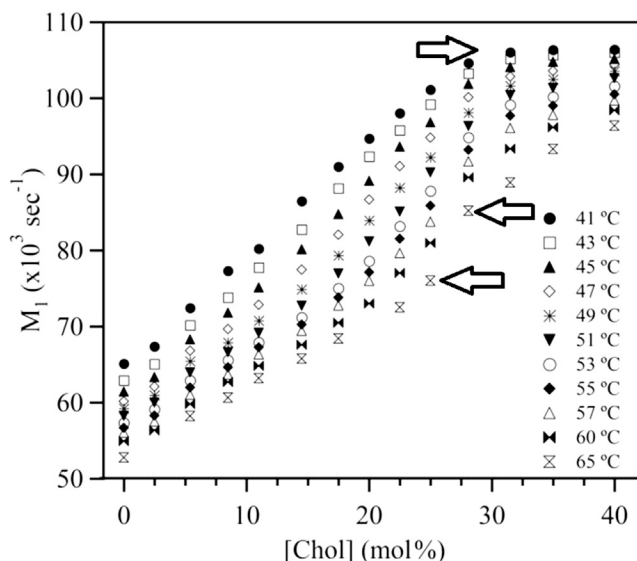
FIGURE 6 First moment (M_1) of PSM-d31/cholesterol spectra as a function of cholesterol concentration for various temperatures above the main transition. Note that the rate of increase in M_1 falls above a certain cholesterol concentration ($\sim$30 mol %) for temperatures <55°C, characteristic of a homogeneous lo phase. Such changes in slope are plotted on the phase diagram in Fig. 7 (top). The right-pointing arrow indicates the ld+lo/lo phase boundary at 41°C (28 mol % cholesterol). The left-pointing arrows indicate the two boundaries, at 25 and 27.5 mol % cholesterol, of the ld+ lo region at 65°C, which is likely close to a critical temperature.

cholesterol. The effect of added cholesterol is less pronounced for lo-phase MLDs. The dependence of M_1 on cholesterol concentration exhibits two distinct behaviors: below 28 mol % cholesterol, the average order parameter increases rapidly, whereas above 28 mol % cholesterol, it increases slowly or levels off. This plateau indicates that the PSM-d31 acyl chain has reached its maximum cholesterol-induced order. The NMR spectra suggest that from 41 to 65°C, 75:25 PSM-d31/cholesterol MLDs have coexisting ld+lo phases, whereas 68.5:31.5 PSM-d31/cholesterol MLDs are in the lo phase. Therefore, the changes of slope in the M_1 (cholesterol) curve suggest an ld+lo/lo boundary near 28 mol % cholesterol. To determine this boundary, a line was drawn through points between 17.5 and 25 mol % cholesterol and another line was fitted to the points between 31.5 and 40 mol % cholesterol. The ld+lo/lo boundary is then obtained from the intercept of the two lines. An alternative approach to map the ld+lo/lo boundary is to examine the behavior of the order parameter of a specific C-D bond. This was verified by analyzing, at several temperatures, the increase in the C12 order parameter with additional cholesterol (Fig. S4).

In principle, there should be a similar change in the slope of M_1 at low cholesterol concentrations, reflecting a crossing of the ld/ld+lo phase boundary. However, no change in slope is observed up to 50°C. For higher temperatures, this slope change becomes obvious and the ld/ld+lo boundary can be determined. The two cholesterol concentrations corresponding to the slope changes come together as the temperature is raised, indicating that the ld/ld+lo and ld+lo/lo boundaries are starting to merge. There is a narrow ld+lo region between 25 and 28 mol % cholesterol at 65°C, suggesting that this temperature is close to the critical point of the PSM-d31/cholesterol MLD. For all temperatures below 55°C, the ld/ld+lo phase boundary was determined by direct examination of the dePaked spectra. The blurred individual peaks at intermediate cholesterol concentrations become sharp again at cholesterol concentrations of 31.5 mol % and above. Thus, the ld/ld+lo phase boundary lies between 8.5 and 25 mol % cholesterol and the ld+lo/lo phase boundary between 28 and 31.5 mol % cholesterol.

Phase diagrams

The partial phase diagrams for PSM-d31/cholesterol and DPPC-d31/cholesterol MLDs determined from the analysis of ^{2}H NMR spectra for various temperatures and cholesterol compositions, as discussed above, are shown in Fig. 7. We have identified three regions of two-phase coexistence and a three-phase line in PSM-d31/cholesterol MLDs and confirmed these features in DPPC-d31/cholesterol MLDs. The region of so and ld phase coexistence lies in a narrow temperature range just below the melting point of the pure lipids and extends up to $\sim$8 mol % cholesterol. The boundaries of this two-phase region were estimated by inspection of the powder spectra as a function of temperature (Fig. 3). The boundaries of the so and lo phase coexistence region were mapped using the well-established spectral subtraction method described in the Supporting Material. For PSM-d31/cholesterol MLDs, the so+lo phase coexistence region lies below 37°C and extends from 9 mol % cholesterol to 27–31 mol % cholesterol. For DPPC-d31/cholesterol MLDs, this region lies below 39°C and extends from 9 mol % cholesterol to 26–30 mol % cholesterol. The so+lo/lo boundary obtained from spectral subtraction is consistent with the onset of the transition in the $M_1(T)$ curves (Fig. 2) for MLDs having cholesterol concentrations $\geq$ 25 mol%.

The ld/ld+lo boundary is determined from the onset of line broadening characteristic of ld+lo heterogeneities in the dePaked spectra, as shown in Fig. 5. The ld+lo/lo boundary in Fig. 7 is determined from the changes of slope in the curves of M_1 versus cholesterol concentration (Fig. 6). For PSM/cholesterol MLDs, the ld/ld+lo boundary shifts from 8 to 22 mol % cholesterol with increasing temperature, whereas the ld+lo/lo boundary, at 28–30 mol % cholesterol, is relatively insensitive to temperature. In the DPPC/cholesterol phase diagram, the ld/ld+lo boundary similarly shifts from 7 to 22 mol % cholesterol with increasing temperature, but the ld+lo/lo boundary has a greater variation, from 26 to 32 mol % cholesterol. The fact that no more than 30 mol % cholesterol is needed to form the lo phase in PSM/cholesterol MLDs could well reflect the known
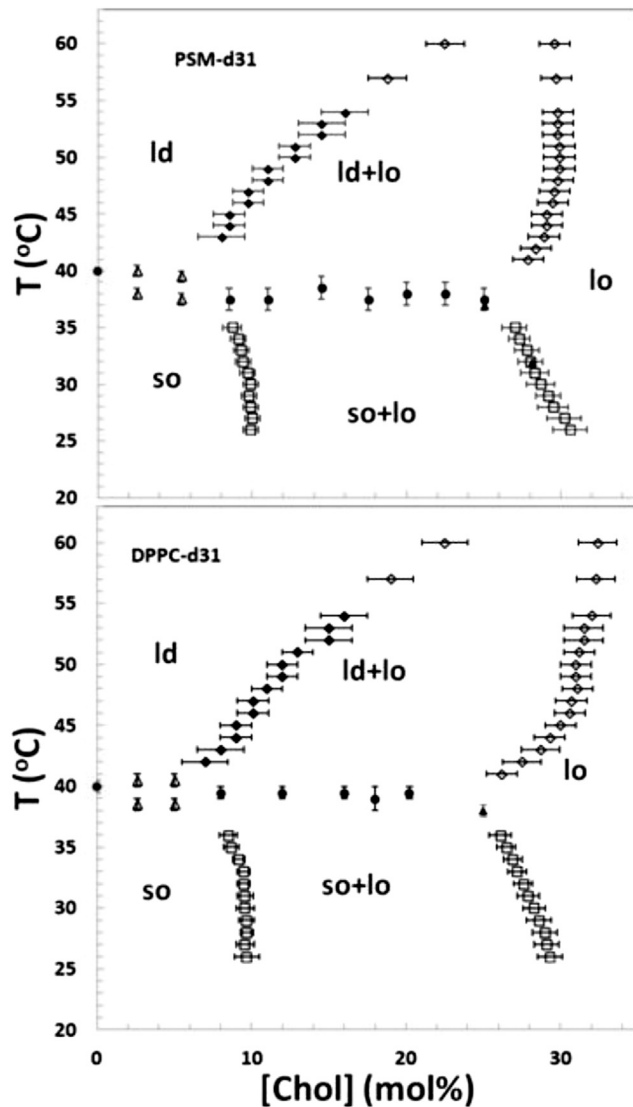
FIGURE 7 Partial phase diagram of PSM-d31/cholesterol (*top*) and DPPC-d31/cholesterol membranes (*bottom*). Symbols indicate the midpoint of the transition, from inspection of dePaked spectra versus temperature (Fig. S3) (*solid circles*); the onset or end of the transition as obtained by inspection of the spectra versus temperature (Fig. 3) (*open triangles*), by spectral subtraction (*open squares*), from M_1(cholesterol) curves (Fig. 6) (*open diamonds*), and by inspection of the dePaked spectra versus cholesterol concentration (Fig. 5) (*solid diamonds*); the onset of the transition in $M_1(T)$ curves for MLDs having cholesterol concentrations of 25 or 28.1 mol % in PSM-d31/cholesterol and 25 mol % in DPPC-d31/cholesterol (*solid triangles*).

higher affinity of cholesterol for PSM than for DPPC (2). The upper bound of the ld+lo phase-coexistence region lies in the vicinity of 65°C in the PSM-d31/cholesterol phase diagram, as discussed above, and higher than 65°C in the DPPC-d31/cholesterol phase diagram.

The so to ld transition for PSM-d31/cholesterol MLDs containing 8.5–25.0 mol % cholesterol was determined by inspecting the dePaked spectrum as a function of temperature between 33 and 43°C (Supporting Material,

Fig. S3). This transition occurs at $T_m = 37.5 \pm 1.0°C$, implying the existence of a three-phase so+lo+ld line separating the so+lo and ld+lo regions in the phase diagram. The temperature of the three-phase line in the DPPC-d31/cholesterol phase diagram was determined, consistently, from both the $M_1(T)$ curves in Fig. 2 and inspection of dePaked spectra as a function of temperature (Fig. S3), to be $T_m = 39.5 \pm 0.5°C$. It lies between 8.0 and 20.5 mol % cholesterol. Note that it is likely that the three-phase line extends to 22.5 mol % cholesterol, but this was not specifically tested.

It is important to emphasize that the phase diagram's shape (Fig. 7) relies heavily on the existence of an isothermal three-phase line separating the so+lo and ld+lo regions. Since this transition temperature cannot be exactly determined, it is possible that this line is not exactly isothermal. If it slopes, even slightly, ld and lo phases are not required to coexist in the region above the line, but the membrane can still display dynamic compositional heterogeneity due to fluctuations.

We now compare the partial phase diagram of *sn*-2-chain-labeled DPPC-d31/cholesterol MLDs with that of DPPC-d62/cholesterol MLDs by Vist and Davis (18). Both diagrams contain a three-phase line and three two-phase regions. For DPPC-d62 MLDs, the main phase transition temperature, T_m, is two degrees lower at 38°C, since both lipid chains are perdeuterated, and in the presence of cholesterol, the so+ld region and the three-phase line occur at lower temperatures for the same reason. To compare the so/(so+lo)/lo boundaries, we consider our spectral subtraction results without the correction due to transverse relaxation time, since this effect is missing in the DPPC-d62/cholesterol study. The so/so+lo boundary lies close to 9 mol % for DPPC-d31/cholesterol MLDs and around 7.5 mol % for DPPC-d62/cholesterol MLDs, which is consistent within error. However, the so+lo/lo boundaries are quite different. The so+lo/lo boundary of DPPC-d62/cholesterol occurs around 22.5 mol % and is nearly vertical, indicating that the amount of cholesterol required to eliminate the last so domains in the so+lo membrane depends only slightly on temperature. In contrast, this boundary is ~5 mol % higher for DPPC-d31/cholesterol MLDs and shifts gradually from 26 mol % at 36°C to 29 mol % at 26°C. The ld/(ld+lo) and (ld+lo)/lo boundaries of DPPC-d62/cholesterol MLDs were partially determined from the upper limit of the broad component of differential scanning calorimetry traces and the sharpening of spectral resonances at high cholesterol concentrations, respectively. The available data above the T_m in (18) agree closely with our work, which extends the phase diagram to considerably higher temperatures.

We also compare the partial phase diagram of PSM-d31/cholesterol MLDs (or DPPC-d31/cholesterol MLDs) with that of *sn*-1-chain-labeled DPPC-d31/ergosterol MLDs determined by Hsueh et al. (20). The overall phase diagrams

are very similar, except that the ld+lo/lo boundary in DPPC-d31/ergosterol MLDs is shifted to lower sterol concentrations and extends only to ~54°C.

Order parameter profile

The ^{2}H NMR spectra of PSM-d31/cholesterol MLDs are much broader than those of DPPC-d31/cholesterol MLDs in both the ld and lo phases (Fig. 1), indicating that the lipid molecules in the two systems have different packing properties. To discuss these differences, we have calculated the order parameter profiles, S_{CD}, along the acyl chains of both lipids for various cholesterol concentrations. Fig. 8 A shows order parameter profiles of PSM-d31/cholesterol MLDs for various cholesterol compositions at 47°C. In pure PSM-d31 MLDs, the S_{CD} is ~0.26 in the plateau region near the headgroup and drops significantly to ~0.02 for the methyl group at the end of the chain. The PSM-d31 plateau S_{CD} of 0.26 compares well with the maximum S_{CD} of 0.24 observed for selectively deuterated stearoylsphingomyelin at 50°C (48). Adding cholesterol orders the membrane at different rates in the ld, ld+lo, and lo regions of the phase diagram. The average order parameter, $<S_{CD}>$, is the average of the individual S_{CD}s that make up the order parameter profile (Fig. 8), excluding the C2 deuterons (see below). It increases from 0.195 to 0.230 in the ld phase when 8.5 mol % cholesterol is added to pure PSM-d31. In the ld+lo region, adding 8 mol % cholesterol to PSM-d31/cholesterol 85.5:14.5 MLDs causes $<S_{CD}>$ to increase much more, from 0.259 to 0.308. In the lo phase, $<S_{CD}>$ increases by only a small amount, from 0.343 to 0.348, when 8.5 mol % cholesterol is added to PSM-d31/cholesterol 68.5:31.5 MLDs. Thus, additional cholesterol is least effective in ordering the lipid chains of PSM-d31 MLDs in the lo phase. This is consistent with the observed reduction in slope at high cholesterol concentrations observed in Fig. 6.

Fig. 8 B shows the order parameter profile of PSM-d31/cholesterol MLDs compared with that of DPPC-d31/cholesterol MLDs for 0, 20, and 40 mol % cholesterol MLDs at 47°C. In the absence of cholesterol, PSM MLDs ($<S_{CD}> = 0.195$) are significantly more ordered than DPPC MLDs ($<S_{CD}> = 0.169$). This result supports the hypothesis of intermolecular hydrogen bonding within the PSM bilayer mediated by the free hydroxyl group of adjacent PSM molecules (49). Fig. 8 B also shows that when cholesterol is added to pure lipids, PSM-d31/cholesterol MLDs are still more ordered than DPPC-d31/cholesterol MLDs, but the difference in the order parameter decreases as cholesterol concentration is increased. For instance, for carbon 10 on the acyl chain, the differences between the S_{CD} of PSM-d31/cholesterol MLDs and that of DPPC-d31/cholesterol MLDs are as follows: for pure lipids, $\Delta S_{CD} = 0.221–0.191 = 0.03$ (PSM 15.7% more ordered than DPPC), for lipids with 20 mol % cholesterol, $\Delta S_{CD} = 0.323–0.298 = 0.025$ (8.4% more ordered) and for MLDs with 40 mol % cholesterol, $\Delta S_{CD} = 0.386–0.365 = 0.021$ (5.7% more ordered). This trend agrees well with the observation that the order parameter profiles of 1:1 mixtures of selectively deuterated stearoylsphingomyelin:cholesterol or 1-palmitoyl-2-stearoyl-*sn*-glycero-3-phosphocholine:cholesterol are almost identical (48).

It should be emphasized that the kink conformation has a unique geometry that is reflected in the reduced quadrupolar splittings of the C2 deuterons (50). One of the C2 deuterons displays unusual behavior as cholesterol is added to the PSM-d31 or DPPC-d31 MLDs (Figs. 5 and 8), indicating that C2 undergoes a unique conformational change. The dePaked spectra of PSM-d31/cholesterol MLDs (Fig. 5) show that the quadrupolar splitting of this C2 deuteron, unlike that of the rest of the acyl chain, drops slightly when cholesterol is added. This quadrupolar splitting changes from ~19 kHz in pure PSM-d31 MLDs to ~16 kHz in PSM-d31 with 40 mol % cholesterol. Fig. 8 A shows that the C3 deuterons in PSM-d31/cholesterol MLDs have different quadrupolar splittings and are therefore inequivalent. This is evident in the dePaked spectra of PSM-d31 and PSM-d31 MLDs with low cholesterol concentrations
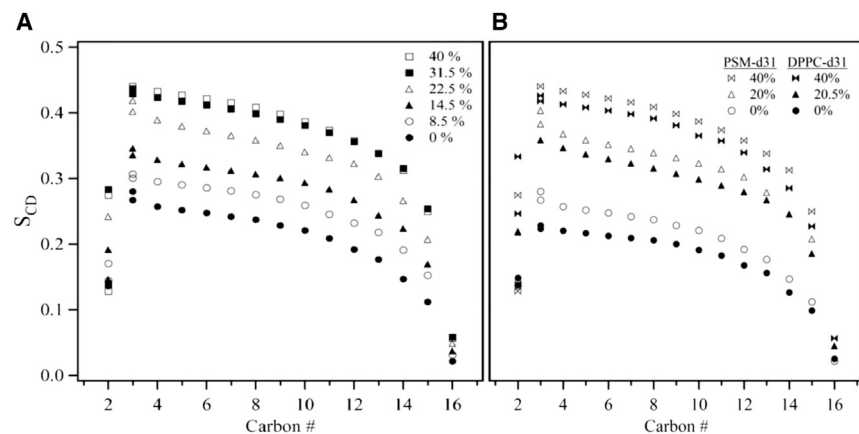

FIGURE 8 Smoothed order parameter profiles of (*A*) PSM-d31/cholesterol and (*B*) PSM-d31/cholesterol and DPPC-d31/cholesterol for various cholesterol concentrations at $T = 47$°C.

(Fig. 5). A similar kink is observed in DPPC-d31/cholesterol MLDs, but the difference in quadrupolar splitting of the C3 deuterons is smaller than that of PSM-d31/cholesterol MLDs.

Domain size in the ld+lo region

Within the ld+lo region, the ^{2}H NMR spectrum of each phase has a different average quadrupolar splitting. For example, the largest quadrupolar splitting in the spectra of PSM-d31 MLDs at 47°C changes from 39.4 kHz at 11 mol % cholesterol to 53.5 kHz at 28 mol %. This difference in quadrupolar splitting translates into an exchange time, τ, of ~46 μs. The translational diffusion constant, D, for PSM/cholesterol bilayers is about $1.8 \times 10^{-12} \text{m}^2/\text{s}$ (34). We used the relation

$$\left(\langle \Delta x^2 \rangle\right)^{1/2} = (4D\tau)^{1/2} \qquad (3)$$

to estimate that a lipid molecule diffuses over a root mean squared (rms) distance of ~18 nm. Domains in the ld+lo region must be much larger than this characteristic distance for the spectrum to show two clearly separable ld and lo components. Our observation of spectral line broadening within this region is instead suggestive of nanoscale separation between cholesterol-rich and cholesterol-poor regions, as was proposed for cell membranes (51), and of the related exchange averaging mechanism. Such small length scales are consistent with the lack of observation of micron-sized phase-separated domains in binary phospholipid/cholesterol GUVs (52).

We now estimate the size of the domains involved in this ld+lo nanoscale phase coexistence by applying the method commonly used to understand A↔B chemical exchange, replacing chemical shifts by quadrupolar splitting (20). The lipid exchange time is

$$\tau = 1/k_{ex}, \qquad (4)$$

where k_{ex} is the rate constant characterizing lipid exchange between the lo and ld domains. This rate constant is obtained from (53)

$$\Delta\delta_{AB} = \Delta\delta_{Q, lo} - \Delta\delta_{Q, ld}, \qquad (6)$$

where $\Delta\delta_{Q,lo}$ and $\Delta\delta_{Q,ld}$ are the quadrupolar splittings of doublets of a particular carbon for the pure ld and lo spectra, respectively. In both PSM/cholesterol and DPPC/cholesterol MLDs, the only isolated doublets for all cholesterol compositions are those for the methyl group and one of the C2 deuterons. However, neither of these peaks is reliable for this calculation. It is well known that the methyl resonance has distinctly long T_1 and T_2 relaxation times, resulting in an inaccurate measurement of its width. In addition, the de-Paked spectra in Fig. 5 show that the quadrupolar splitting of the C2 deuteron in PSM-d31/cholesterol MLDs stays more or less constant as the cholesterol concentration is raised. Our best option is the C15 peak, since it is either well separated from other peaks or overlaps with only one other peak, in which case it can be separated by multipeak fitting.

The rate constants for the relaxation times $T_{2,\text{obs}}$, T_{2A}, and T_{2B} are given by

$$1/T_{2,\text{obs}} = \pi\Delta\nu_{ld+lo} \qquad (7a)$$

$$1/T_{2,A} = \pi\Delta\nu_{lo} \qquad (7b)$$

$$1/T_{2,B} = \pi\Delta\nu_{ld}, \qquad (7c)$$

where $\Delta\nu_{ld+lo}$, $\Delta\nu_{lo}$, and $\Delta\nu_{ld}$ are the widths at half-maximum height of the individual C15 peaks in the depaked ld+lo, lo, and ld spectra, respectively.

The calculation of domain size within the ld+lo region is based on the labeled phospholipids diffusing between the two domains. In principle, the phospholipid and cholesterol molecules all diffuse in the coexistence region. A study of the lateral diffusion of DPPC and cholesterol by ^{1}H pulsed field gradient magic-angle spinning NMR spectroscopy (34) revealed that the diffusion constants of DPPC and cholesterol are very close. For example, in DPPC-d62 bilayers with 20 mol % cholesterol at 47°C, $D = 7.5 \times 10^{-12} \text{m}^2/\text{s}$ for DPPC and $D = 9.0 \times 10^{-12} \text{m}^2/\text{s}$ for cholesterol. Depending on the cholesterol

$$1/T_{2,\text{obs}} = (f_A)/(T_{2A}) + (f_B)/(T_{2B}) + \frac{k_{ex}}{2} - \frac{1}{\sqrt{8}}\left\{k_{ex}^2 - 4\pi^2(\Delta\delta_{AB})^2 + \left[\left(k_{ex}^2 + 4\pi^2(\Delta\delta_{AB})^2\right)^2 - 16f_Af_B4\pi^2(\Delta\delta_{AB})^2k_{ex}^2\right]^{1/2}\right\}^{1/2}. \qquad (5)$$

In this equation, f_A and f_B are fractions of the total labeled lipid in the lo and ld domains, respectively, and $\Delta\delta_{AB} = \Delta\delta_A - \Delta\delta_B$ is the difference of the quadrupolar splittings in the two states,

composition, the DPPC diffusion constant is four to six times larger than that of sphingomyelin (54).

Examples of the parameters required to estimate the rms distance, $\left(\langle \Delta x^2 \rangle\right)^{1/2}$, in DPPC/cholesterol, PSM/cholesterol,

and DPPC/ergosterol MLDs (20) are listed in Table 1. The rms distance reported by Hsueh et al. (20) is roughly one-sixth that of DPPC/cholesterol MLDs. The main discrepancy arises from their explicit assumption that the lipid molecules undergo fast exchange between the two domains. Under this condition, Eq. 5, which is exact, reduces to the approximate solution for k_{ex} used by Hsueh et al. Our comparison between exact and approximate equations results in domain sizes that differ by an order of magnitude. This indicates that in our case, the labeled phospholipids undergo intermediate exchange; hence, the exact equation must be used. We also compare our results with the work by Veatch et al. (55), who estimated domain sizes of ∼80 nm in GUVs made up of dioleoylphosphatidylcholine/DPPC (1:1) + 30 mol % cholesterol that display liquid/liquid coexistence at 25°C.

The exchange rate was obtained by solving Eq. 5 numerically and is plotted in Fig. 9 A. At 20 mol % cholesterol, the exchange times for PSM-d31 and DPPC-d31 molecules between the ld and lo phases are ∼200 and ∼60 μs, respectively.

The domain size in the ld+lo region is considered double the rms distance, and its dependence on cholesterol concentration is illustrated in Fig. 9 B. The size of the domains for PSM-d31/cholesterol and DPPC/cholesterol MLDs are in the nanoscale regime and in close agreement with each other. Note that close to the ld and lo boundaries, the domains enlarge significantly, indicating that the membrane is becoming more homogeneous. The number of molecules constituting a domain is not known, since we have no information on domain shape. If we assume that the domains are circular, the number of DPPC molecules constituting an **ld** domain close to the middle of the **ld+lo** region is on the order of 10^4, since each DPPC molecule occupies ∼0.60 nm^2 (27,56,57).This implies that there are ∼9000 DPPC molecules and ∼1000 cholesterol molecules in an ld domain of diameter 90 nm.

Fluorescence microscopy methods have not been able to detect the phase separations in binary DPPC-cholesterol mixtures that have been inferred from ^{2}H NMR studies. The line broadening observed in DPPC/cholesterol MLDs (18), DPPC/ergosterol MLDs (20), and the binary MLDs

studied in this work was attributed to a diffusion-limited exchange of lipids between domains of the coexisting liquid phases. More recently Shaghaghi et al. (58) observed similar broadening in various POPC/phytosterol MLDs.

The "condensed complex" model (CCM) provides an alternative interpretation for phase diagrams involving sterols and, in particular, for domain formation (line broadening) in DPPC/cholesterol and DPPC/ergosterol binary mixtures (59). The CCM is a thermodynamic model that attributes the composition-dependent NMR line broadening to the kinetics of complex formation between these sterols and DPPC molecules (28). Micron-sized immiscible liquid domains have been observed in ternary mixtures of DPPC/DOPC/cholesterol by fluorescence microscopy (60). The CCM provides a semi-quantitative description of the DPPC/DOPC/cholesterol phase diagram and involves no phase separation of DPPC/cholesterol or other binary lipid systems. In particular, the chemical kinetics of complex formation and dissociation is able to account for the ^{2}H NMR line broadening attributed to nanoscale domain coexistence. The calculated first moment of the ^{2}H NMR spectra in DPPC/ergosterol MLDs using the parameters in the model fits well with the experimental data (20). However, a more recent study on DPPC/DiPhyPC/cholesterol ternary mixtures using the CCM predicts phase separations in binary DPPC/cholesterol mixtures (29). Thus, although dynamic "condensed complexes" are useful for modelling the phase diagrams of lipid systems, the choice of model parameters strongly influences the prediction of phase separation in binary mixtures.

CONCLUSIONS

We have constructed and compared partial phase diagrams for N-linked palmitoyl-chain-perdeuterated PSM-d31/cholesterol and *sn-2*-palmitoyl-chain-perdeuterated DPPC-d31/cholesterol MLDs solely from ^{2}H NMR measurements. It was found that these phase diagrams are very similar. They both exhibit so+lo and ld+lo coexistence regions with a clear three-phase line separating them. In both phase diagrams, the narrowing of the ld+lo coexistence region at high temperature implies that a critical point

TABLE 1 Parameters Used in Eqs. 3, 4, and 5 and the Estimated rms Length Scale, $(\langle \Delta x^2 \rangle)^{1/2}$, Characterizing the ld/lo Domains

Parameters and Results	DPPC-d31/Cholesterol	PSM-d31/Cholesterol	DPPC-d31/Ergosterol
Cholesterol mol %	20.5	20	20
D	7.5×10^{-12} m^2/s	1.8×10^{-12} m^2/s	10^{-11} m^2/s
f_A	0.44	0.45	0.52
f_B	0.56	0.55	0.48
$1/T_{2A}$	3.4 $(ms)^{-1}$	3.4 $(ms)^{-1}$	3.8 $(ms)^{-1}$
$1/T_{2B}$	5.7 $(ms)^{-1}$	4.5 $(ms)^{-1}$	3.2 $(ms)^{-1}$
$1/T_{2,obs}$	7.6 $(ms)^{-1}$	6.8 $(ms)^{-1}$	7.1 $(ms)^{-1}$
$\Delta\nu_{Q,lo}$	56.2 kHz	64.4 kHz	53.4 kHz
$\Delta\nu_{Q,ld}$	33.6 kHz	34.6 kHz	27.8 kHz
$\Delta\delta_{AB}$	22.6 kHz	29.8 kHz	25.6 kHz
$(<\Delta x^2>)^{1/2}$	44 nm	38 nm	6.5 nm

Temperature and cholesterol concentration were kept constant at $T = 47°C$ and 20 mol %, respectively.
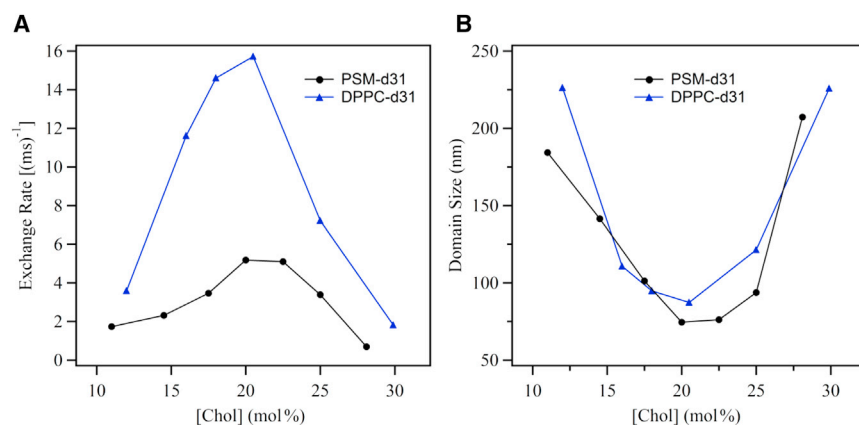
FIGURE 9 (*A*) The NMR exchange rate and (*B*) the domain size for PSM-d31/cholesterol and DPPC-d31/cholesterol membranes within the ld+lo region for various cholesterol compositions at $T = 47°C$. To see this figure in color, go online.

exists corresponding to a cholesterol concentration between ~25 and 30 mol %. By relaxing the requirement of fast lipid exchange, we were able to characterize the ld+lo nanodomain coexistence region with improved accuracy compared with previous studies (20). We estimated distances between ld/lo domain interfaces in PSM/cholesterol and DPPC/cholesterol MLDs to be ~80 nm. Such dimensions are on the order of the purported size of "rafts" in cell membranes (61). Thus, if rafts exist in cell membranes they will be strongly influenced by lipid/lipid interactions. The high cholesterol concentration found in many plasma membranes, however, makes it likely that their preferred physical organization is similar to the lo phase. Complicating matters in biological membranes is the asymmetric distribution of lipid molecules between the inner and outer leaflets. Cholesterol distribution is still controversial; recently, a ratio of 12:1 outer/inner leaflet cholesterol concentration in HeLa cell plasma membranes was observed, and this asymmetry was attributed to sphingomyelin "trapping" cholesterol in the outer leaflet (62).

Although the physical organization of PSM and DPPC membranes is not grossly different, nature chooses to use PSM instead of DPPC in most natural cell membranes. In the liquid crystalline (ld) phase, pure PSM MLDs are significantly more ordered than pure DPPC MLDs, but this difference diminishes as cholesterol is added. This implies that it takes less cholesterol to promote an lo phase in PSM MLDs than in DPPC MLDs. In other words, cholesterol orders PSM lipid chains more effectively than DPPC acyl chains to form an lo phase. This is consistent with our observation that above 45°C, the ld+lo/lo boundary in the PSM/cholesterol phase diagram forms at a lower cholesterol concentration (by ~2 mol %) than in the DPPC/cholesterol phase diagram.

The outer leaflet of plasma membrane is mostly composed of sphingomyelin, POPC, and cholesterol. The next logical step in determining the lipid-lipid interactions governing possible raft formation is to study ternary mixtures of PSM/POPC/cholesterol, ideally deuterating each lipid, including cholesterol, in turn. This ternary system has already been explored by fluorescence microscopy techniques and ^{2}H NMR (2,10,32,33). Results consistently show micron-scale phase separation at temperatures below 40°C, but this system is not so well characterized at higher temperatures. Bunge et al. (33) studied 3:3:2 PSM/POPC/cholesterol mixtures at 40°C and reported evidence of inhomogeneous cholesterol distribution, but they observed no micron-scale domains. Now that we have a detailed picture of the PSM/cholesterol binary system, ^{2}H NMR can be used to study the ternary system more thoroughly and thus gain insight into the complex behavior of lipid rafts in cellular plasma membranes.

SUPPORTING MATERIAL

Supporting Materials and Methods, Supporting Results and Discussion, four figures, and one table are available at http://www.biophysj.org/biophysj/supplemental/S0006-3495(18)30150-4.

AUTHOR CONTRIBUTIONS

A.K. designed research, performed research, contributed analytic tools, analyzed data, and wrote the article. M.S. performed research, analyzed data, and wrote the article. M.J.Z. designed research and wrote the article. J.T. designed research, wrote the article, and takes primary responsibility for the final content.

ACKNOWLEDGMENTS

REFERENCES

1. Lozano, M. M., J. S. Hovis, …, S. G. Boxer. 2016. Dynamic reorganization and correlation among lipid raft components. *J. Am. Chem. Soc.* 138:9996–10001.

2. Engberg, O., V. Hautala, …, T. K. M. Nyholm. 2016. The affinity of cholesterol for different phospholipids affects lateral segregation in bilayers. *Biophys. J.* 111:546–556.

3. Sodt, A. J., R. M. Venable, …, R. W. Pastor. 2016. Nonadditive compositional curvature energetics of lipid bilayers. *Phys. Rev. Lett.* 117:138104.

4. Quinn, P. J. 2013. Structure of sphingomyelin bilayers and complexes with cholesterol forming membrane rafts. *Langmuir.* 29:9447–9456.

5. Alwarawrah, M., J. Dai, and J. Huang. 2010. A molecular view of the cholesterol condensing effect in DOPC lipid bilayers. *J. Phys. Chem. B.* 114:7516–7523.

6. Dai, J., M. Alwarawrah, …, J. Huang. 2011. Simulation of the lo-ld phase boundary in DSPC/DOPC/cholesterol ternary mixtures using pairwise interactions. *J. Phys. Chem. B.* 115:1662–1671.

7. Zachowski, A. 1993. Phospholipids in animal eukaryotic membranes: transverse asymmetry and movement. *Biochem. J.* 294:1–14.

8. Murate, M., M. Abe, …, T. Kobayashi. 2015. Transbilayer distribution of lipids at nano scale. *J. Cell Sci.* 128:1627–1638.

9. Ahmed, S. N., D. A. Brown, and E. London. 1997. On the origin of sphingolipid/cholesterol-rich detergent-insoluble cell membranes: physiological concentrations of cholesterol and sphingolipid induce formation of a detergent-insoluble, liquid-ordered lipid phase in model membranes. *Biochemistry.* 36:10944–10953.

10. Veatch, S. L., and S. L. Keller. 2005. Miscibility phase diagrams of giant vesicles containing sphingomyelin. *Phys. Rev. Lett.* 94:148101.

11. de Almeida, R. F. M., A. Fedorov, and M. Prieto. 2003. Sphingomyelin/phosphatidylcholine/cholesterol phase diagram: boundaries and composition of lipid rafts. *Biophys. J.* 85:2406–2416.

12. Sahl, S. J., M. Leutenegger, …, C. Eggeling. 2010. Fast molecular tracking maps nanoscale dynamics of plasma membrane lipids. *Proc. Natl. Acad. Sci. USA.* 107:6829–6834.

13. Frisz, J. F., K. Lou, …, M. L. Kraft. 2013. Direct chemical evidence for sphingolipid domains in the plasma membranes of fibroblasts. *Proc. Natl. Acad. Sci. USA.* 110:E613–E622.

14. Das, A., J. L. Goldstein, …, A. Radhakrishnan. 2013. Use of mutant ^{125}I-perfringolysin O to probe transport and organization of cholesterol in membranes of animal cells. *Proc. Natl. Acad. Sci. USA.* 110:10580–10585.

15. Carquin, M., H. Pollet, …, D. Tyteca. 2014. Endogenous sphingomyelin segregates into submicrometric domains in the living erythrocyte membrane. *J. Lipid Res.* 55:1331–1342.

16. Carquin, M., L. Conrard, …, D. Tyteca. 2015. Cholesterol segregates into submicrometric domains at the living erythrocyte membrane: evidence and regulation. *Cell. Mol. Life Sci.* 72:4633–4651.

17. Vecer, J., P. Vesela, …, P. Herman. 2014. Sphingolipid levels crucially modulate lateral microdomain organization of plasma membrane in living yeast. *FEBS Lett.* 588:443–449.

18. Vist, M. R., and J. H. Davis. 1990. Phase equilibria of cholesterol/dipalmitoylphosphatidylcholine mixtures: [2]H nuclear magnetic resonance and differential scanning calorimetry. *Biochemistry.* 29:451–464.

19. Juhasz, J., J. H. Davis, and F. J. Sharom. 2012. Fluorescent probe partitioning in GUVs of binary phospholipid mixtures: implications for interpreting phase behavior. *Biochim. Biophys. Acta.* 1818:19–26.

20. Hsueh, Y. W., K. Gilbert, …, J. Thewalt. 2005. The effect of ergosterol on dipalmitoylphosphatidylcholine bilayers: a deuterium NMR and calorimetric study. *Biophys. J.* 88:1799–1808.

21. Veatch, S. L., O. Soubias, …, K. Gawrisch. 2007. Critical fluctuations in domain-forming lipid mixtures. *Proc. Natl. Acad. Sci. USA.* 104:17650–17655.

22. Ipsen, J. H., G. Karlström, …, M. J. Zuckermann. 1987. Phase equilibria in the phosphatidylcholine-cholesterol system. *Biochim. Biophys. Acta.* 905:162–172.

23. Ali, M. R., K. H. Cheng, and J. Huang. 2007. Assess the nature of cholesterol-lipid interactions through the chemical potential of cholesterol in phosphatidylcholine bilayers. *Proc. Natl. Acad. Sci. USA.* 104:5372–5377.

24. Pandit, S. A., and H. L. Scott. 2009. Multiscale simulations of heterogeneous model membranes. *Biochim. Biophys. Acta.* 1788:136–148.

25. Longo, G. S., M. Schick, and I. Szleifer. 2009. Stability and liquid-liquid phase separation in mixed saturated lipid bilayers. *Biophys. J.* 96:3977–3986.

26. Róg, T., A. Orłowski, …, I. Vattulainen. 2016. Interdigitation of long-chain sphingomyelin induces coupling of membrane leaflets in a cholesterol dependent manner. *Biochim. Biophys. Acta.* 1858:281–288.

27. Greenwood, A. I., S. Tristram-Nagle, and J. F. Nagle. 2006. Partial molecular volumes of lipids and cholesterol. *Chem. Phys. Lipids.* 143:1–10.

28. McConnell, H. M., and A. Radhakrishnan. 2003. Condensed complexes of cholesterol and phospholipids. *Biochim. Biophys. Acta.* 1610:159–173.

29. Radhakrishnan, A. 2010. Phase separations in binary and ternary cholesterol-phospholipid mixtures. *Biophys. J.* 98:L41–L43.

30. Goñi, F. M., A. Alonso, …, J. L. Thewalt. 2008. Phase diagrams of lipid mixtures relevant to the study of membrane rafts. *Biochim. Biophys. Acta.* 1781:665–684.

31. García-Arribas, A. B., A. Alonso, and F. M. Goñi. 2016. Cholesterol interactions with ceramide and sphingomyelin. *Chem. Phys. Lipids.* 199:26–34.

32. Bartels, T., R. S. Lankalapalli, …, M. F. Brown. 2008. Raftlike mixtures of sphingomyelin and cholesterol investigated by solid-state ^{2}H NMR spectroscopy. *J. Am. Chem. Soc.* 130:14521–14532.

33. Bunge, A., P. Müller, …, D. Huster. 2008. Characterization of the ternary mixture of sphingomyelin, POPC, and cholesterol: support for an inhomogeneous lipid distribution at high temperatures. *Biophys. J.* 94:2680–2690.

34. Filippov, A., G. Orädd, and G. Lindblom. 2003. The effect of cholesterol on the lateral diffusion of phospholipids in oriented bilayers. *Biophys. J.* 84:3079–3086.

35. Collado, M. I., F. M. Goñi, …, D. Marsh. 2005. Domain formation in sphingomyelin/cholesterol mixed membranes studied by spin-label electron spin resonance spectroscopy. *Biochemistry.* 44:4911–4918.

36. Muhr, P., W. Likussar, and M. Schubert-Zsilavecz. 1996. Structure investigation and proton and carbon-13 assignments of digitonin and cholesterol using multidimensional NMR techniques. *Magn. Reson. Chem.* 34:137–142.

37. Peng, X., A. Jonas, and J. Jonas. 1995. One and two dimensional ^{1}H-NMR studies of pressure and tetracaine effects on sonicated phospholipid vesicles. *Chem. Phys. Lipids.* 75:59–69.

38. Davis, J. H., K. R. Jeffrey, …, T. P. Higgs. 1976. Quadrupolar echo deuteron magnetic resonance spectroscopy in ordered hydrocarbon chains. *Chem. Phys. Lett.* 42:390–394.

39. Sternin, E., M. Bloom, and A. L. Mackay. 1983. De-pake-ing of NMR spectra. *J. Magn. Reson.* 55:274–282.

40. Schafer, H., B. Madler, and F. Volke. 1995. De-Pake-ing of NMR powder spectra by nonnegative least-squares analysis with Tikhonov regularization. *J. Magn. Reson. A.* 116:145–149.

41. Lafleur, M., B. Fine, …, M. Bloom. 1989. Smoothed orientational order profile of lipid bilayers by [2]H-nuclear magnetic resonance. *Biophys. J.* 56:1037–1041.

42. Lange, A., D. Marsh, …, G. Kothe. 1985. Electron spin resonance study of phospholipid membranes employing a comprehensive line-shape model. *Biochemistry.* 24:4383–4392.

43. Prosser, R. S., J. H. Davis, …, G. Kothe. 1992. Deuterium NMR relaxation studies of peptide-lipid interactions. *Biochemistry.* 31:9355–9363.

44. Weisz, K., G. Gröbner, …, G. Kothe. 1992. Deuteron nuclear magnetic resonance study of the dynamic organization of phospholipid/cholesterol bilayer membranes: molecular properties and viscoelastic behavior. *Biochemistry.* 31:1100–1112.

45. Trouard, T. P., A. A. Nevzorov, …, M. F. Brown. 1999. Influence of cholesterol on dynamics of dimyristoylphosphatidylcholine bilayers as studied by deuterium NMR relaxation. *J. Chem. Phys.* 110:8802–8818.

46. Davis, J. H. 1986. NMR studies of cholesterol orientational order and dynamics, and the phase equilibria of cholesterol/phospholipid mixtures. *In* Physics of NMR Spectroscopy in Biology and Medicine. B. Maraviglia, ed. North Holland, pp. 302–312.

47. Davis, J. H. 1979. Deuterium magnetic resonance study of the gel and liquid crystalline phases of dipalmitoyl phosphatidylcholine. *Biophys. J.* 27:339–358.

48. Yasuda, T., M. Kinoshita, …, N. Matsumori. 2014. Detailed comparison of deuterium quadrupole profiles between sphingomyelin and phosphatidylcholine bilayers. *Biophys. J.* 106:631–638.

49. Niemelä, P., M. T. Hyvönen, and I. Vattulainen. 2004. Structure and dynamics of sphingomyelin bilayer: insight gained through systematic comparison to phosphatidylcholine. *Biophys. J.* 87:2976–2989.

50. Mehnert, T., K. Jacob, …, K. Beyer. 2006. Structure and lipid interaction of N-palmitoylsphingomyelin in bilayer membranes as revealed by ^{2}H-NMR spectroscopy. *Biophys. J.* 90:939–946.

51. Varma, R., and S. Mayor. 1998. GPI-anchored proteins are organized in submicron domains at the cell surface. *Nature.* 394:798–801.

52. Veatch, S. L., and S. L. Keller. 2003. Separation of liquid phases in giant vesicles of ternary mixtures of phospholipids and cholesterol. *Biophys. J.* 85:3074–3083.

53. Carrington, A., and A. D. McLachlan. 1967. Introduction to Magnetic Resonance. Harper & Row, New York.

54. Lindblom, G., G. Orädd, and A. Filippov. 2006. Lipid lateral diffusion in bilayers with phosphatidylcholine, sphingomyelin and cholesterol. An NMR study of dynamics and lateral phase separation. *Chem. Phys. Lipids.* 141:179–184.

55. Veatch, S. L., I. V. Polozov, …, S. L. Keller. 2004. Liquid domains in vesicles investigated by NMR and fluorescence microscopy. *Biophys. J.* 86:2910–2922.

56. Seelig, J. 1981. Thermodynamics of phospholipid bilayers. *In* Membranes and Intercellular Communication. R. Balian, M. Chabre, and P. F. Devaux, eds. North-Holland, pp. 18–78.

57. Levine, Y. K., and M. H. F. Wilkins. 1971. Structure of oriented lipid bilayers. *Nat. New Biol.* 230:69–72.

58. Shaghaghi, M., M. T. Chen, …, J. L. Thewalt. 2016. Effect of sterol structure on the physical properties of 1-palmitoyl-2-oleoyl-*sn*-glycero-3-phosphocholine membranes determined using ^{2}H nuclear magnetic resonance. *Langmuir.* 32:7654–7663.

59. McConnell, H., and A. Radhakrishnan. 2006. Theory of the deuterium NMR of sterol-phospholipid membranes. *Proc. Natl. Acad. Sci. USA.* 103:1184–1189.

60. Veatch, S. L., and S. L. Keller. 2005. Seeing spots: complex phase behavior in simple membranes. *Biochim. Biophys. Acta.* 1746:172–185.

61. Kusumi, A., I. Koyama-Honda, and K. Suzuki. 2004. Molecular dynamics and interactions for creation of stimulation-induced stabilized rafts from small unstable steady-state rafts. *Traffic.* 5:213–230.

62. Liu, S. L., R. Sheng, …, W. Cho. 2017. Orthogonal lipid sensors identify transbilayer asymmetry of plasma membrane cholesterol. *Nat. Chem. Biol.* 13:268–274.

Supplemental Information

The Phase Behavior and Organization of Sphingomyelin/Cholesterol Membranes: A Deuterium NMR Study

Amir Keyvanloo, Mehran Shaghaghi, Martin J. Zuckermann, and Jenifer L. Thewalt

SUPPLEMENTARY INFORMATION

MATERIALS AND METHODS

^{2}H NMR spectroscopy

Spectral subtraction

The boundaries of the **so + lo** coexistence region are determined by the spectral subtraction method (18). Within this two-phase region, a ^{2}H NMR spectrum consists of different amounts of endpoint spectra characteristic of the two phases in equilibrium and the phase boundaries, x_s and x_f, can be calculated:

$$x_s = \frac{(1 - x_B)x_A - K(1 - x_A)x_B}{(1 - x_B) - K(1 - x_A)} \tag{S1}$$

$$x_f = \frac{(1 - x_A)x_B - K'(1 - x_B)x_A}{(1 - x_A) - K'(1 - x_B)}, \tag{S2}$$

where K is the ratio of **lo**-phase lipid fractions in the two samples, K' is the ratio of **so**-phase lipid fractions in the two samples, and x_A and x_B are the cholesterol concentrations of two lipid/cholesterol MLDs. The spectral subtraction method is valid as long as certain assumptions hold. The spectra of the two phases, S_s and S_f, have to be sufficiently different that one can easily distinguish and carry out the subtraction procedure. The exchange of labeled lipid between two kinds of domains must be slow on the NMR timescale so that it can be neglected. In addition, the domain must be sufficiently large, so that the signal from the lipid on the boundary of the domains is negligible. Also, this method assumes that both phases have the same relaxation time T_{2e}, which is not true in our case. Depending on the temperature, the **lo** phase has a T_{2e} two to six times larger than the **so** phase T_{2e} and therefore the **so** component decays faster than the **lo** component (the signal $\propto e^{-t/T_{2e}}$). Thus, at any given quadrupolar echo time 2τ, the ^{2}H NMR spectrum will contain a smaller **so** component S_s than is representative of the sample. Due to this T_{2e} effect f_A and f_B in Eqs. S1 and S2, which should be denoted as $f_A(t = 2\tau)$ and $f_B(t = 2\tau)$, do not reflect the actual fractions of fluid lipid in the samples. Thus, the K and K' (which should be denoted as $K(t = 2\tau)$ and $K'(t = 2\tau)$, respectively) determined from the spectral subtraction will not be correct, leading to a deviation of x_s and x_f from the actual values. To incorporate this T_{2e} effect, corrected f_A and f_B values (i.e., $f_A(t = 0)$ and $f_B(t = 0)$) are calculated by extrapolating the height of the respective echo signal back to $t = 0$ using the measured T_{2e} for a given temperature, and then the corrected K and K' values (i.e., $K(t = 0)$ and $K'(t = 0)$) can be derived and expressed in terms of the experimentally determined K and K' (i.e., $K(t = 2\tau)$ and $K'(t = 2\tau)$), and T_{2e}s. Assuming the gel component of a mixed spectrum will have decayed by an extra factor R relative to the liquid ordered component, then (R1)

$$K_{t=0} = C\, K_{t=2\tau} \tag{S3}$$

$$K'_{t=0} = \left(\frac{1}{C}\right) K'_{t=2\tau} \tag{S4}$$

where the coefficient C is given by

$$C = \frac{1 + f_A\left(\frac{1 - R}{R}\right)}{1 + f_B\left(\frac{1 - R}{R}\right)} \tag{S5}$$

Using Eqs. S1 and S2 with these corrected K and K' values, the T_{2e}-corrected values of x_s and x_f are obtained.

RESULTS AND DISCUSSION

Phase Boundaries at Higher Cholesterol Content and Low Temperature: so/(so+lo)/lo

Spectral subtraction

Figure S1 illustrates the spectral subtraction procedure at 32°C using normalized spectra of PSM-d31/cholesterol MLDs with 11 and 22.5 mol % cholesterol, Figs. S1A(I) and S1A(II). We refer to the 11 mol % cholesterol membrane as "**so**-rich" and the 22.5 mol % cholesterol membrane as "**lo**-rich". By subtracting 24% of the **so**-rich spectrum from the **lo**-rich spectrum we obtain the difference spectrum shown in Fig. S1A(IV). The value $K' = 0.24$ gives the **lo**-phase end-point mole fraction $x_f = 0.255$ denoting the **so**+**lo**/**lo** boundary. This difference spectrum, renormalized in Fig. S1B(II), is compared with the normalized experimental spectrum obtained at 31°C for 25 mol % cholesterol, Fig. S1B(I). The difference between the spectra in Figs. S1B(I) and S1B(II) is shown in Fig. S1B(III). Clearly, there is excellent agreement between the end-point spectrum obtained by spectral subtraction and the spectrum of the 25 mol % sample. If we subtract 17% of the **lo**-rich spectrum from the **so**-rich spectrum, then we obtain the **so**-phase end-point spectrum shown in Fig. S1A(III), corresponding to a cholesterol mole fraction of $x_s = 0.082$. This difference spectrum, after normalization (Fig. S1B(V)), is compared to the experimental spectrum obtained for the 8.5 mol % sample at 31°C (Fig. S1B(IV)). The difference between the end-point spectrum and the 8.5 mol % spectrum is shown in Fig. S1B(VI). The spectral subtraction approach thus proves robust in separating experimental spectra of MLDs within the **so**+**lo** region into their end-point components. Errors in determining the end-point cholesterol mole fractions resulted from the uncertainty in K and K' values for a given pair of experimental spectra in the **so**+**lo** coexistence region.
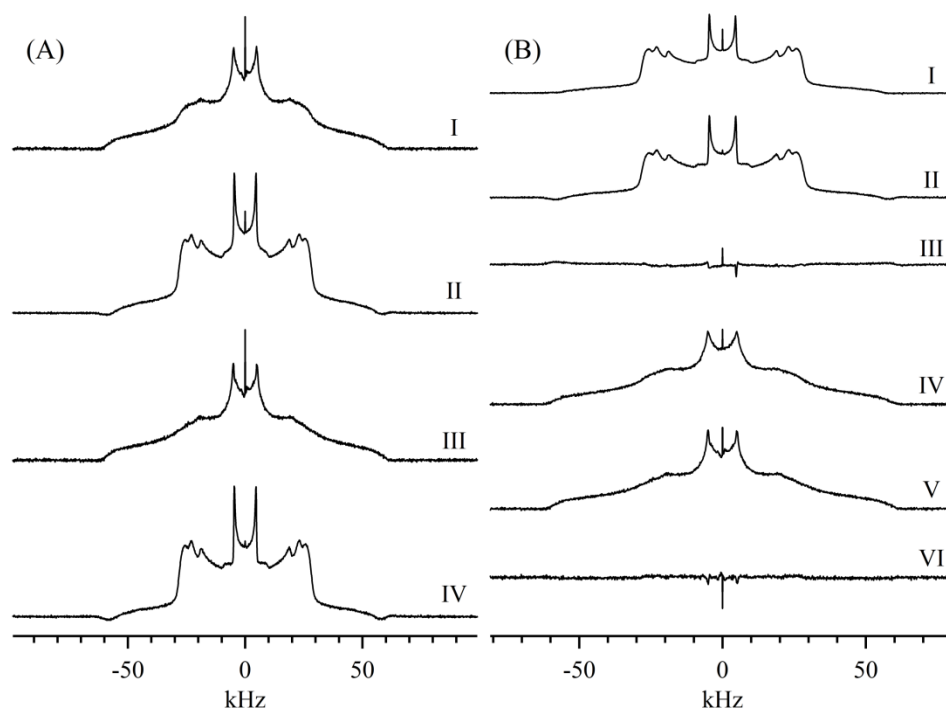
Figure S1: ^{2}H NMR spectral subtraction at 32°: (A)I and (A)II show experimental spectra of 11 mole% and 22.5 mol% cholesterol, respectively; (A)III displays the spectrum in (A)I minus 0.17 times that in (A)II; (A)IV displays the spectrum in (A)II minus 0.24 times that in (A)I. Figure S1(B) compares the end-point difference spectra with experimental spectra at 32°C: (B)I is the spectrum of the 25 mol% cholesterol sample; (B)II is the end-point difference spectrum in (A)IV; (B)III is the difference between the spectra in (B)I and (B)II; (B)IV is the spectrum of the 8.5 mol% cholesterol sample; (B)V is the end-point difference spectrum in (A)III; (B)VI is the difference between the spectra in (B)IV and (B)V. All spectra (except those in (B)III and (B)VI) are normalized in area.

As was discussed in the Materials and Methods section, the spectral subtraction procedure assumes that the **so** and **lo** phases have the same relaxation time, T_{2e}. Figure S2 shows that this is not true for PSM-d31/cholesterol; depending on the temperature the **lo** phase has a T_{2e} two to six times longer than that of the **so** phase. Thus the **so** component decays faster than the **lo** component and is underrepresented in the quadrupolar echo spectrum of a membrane containing both phases. Note that 5.4 and 35 mol % cholesterol compositions are used to measure relaxation times of the **so** and **lo** phases, respectively. The values of the end-point compositions, x_s and x_f, with and without T_{2e} correction are listed in Table S1. At each temperature there is a significant shift of 2.5±0.4 mol % in the **so**+**lo**/**lo** boundary to higher cholesterol concentrations. A less dramatic shift of <1.2 mol % is observed for DPPC-d31/cholesterol. Furthermore, for both PSM-d31/cholesterol and DPPC-d31/cholesterol a relatively small shift in the **so**/**so**+**lo** boundary is observed, ranging from 0.3 to 1.8 mole%.
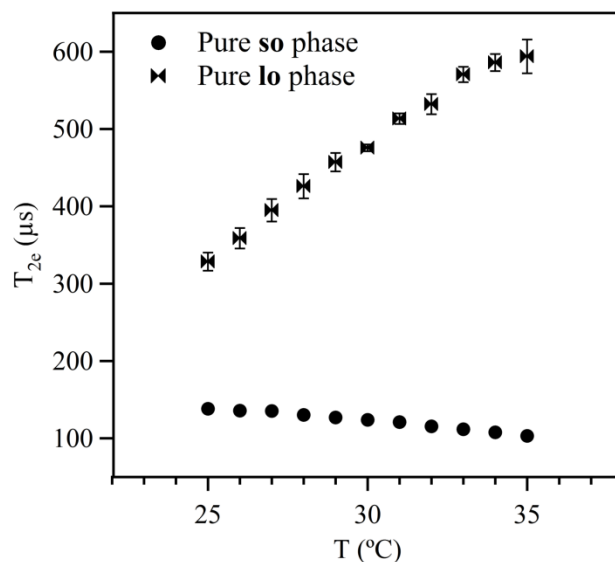
Figure S2: T_{2e} as a function of temperature for PSM-d31/cholesterol membranes with 5.4 mol% cholesterol (pure **so** phase) and 35 mol% cholesterol (pure **lo** phase).

Table S1: Comparison of the x_s and x_f values and those with T_{2e} corrections.

T (°C)	No Correction		With T_{2e} Correction	
	x_s	x_f	x_s	x_f
27	9.7 ± 0.5	27.3 ± 0.8	10 ± 0.5	30.2 ± 1.1
29	9.2 ± 0.4	26.4 ± 0.5	9.8 ± 0.5	29.2 ± 0.8
31	9 ± 0.5	25.7 ± 0.7	9.7 ± 0.5	28.3 ± 0.9
33	8 ± 0.6	25.3 ± 0.6	9.3 ± 0.5	27.8 ± 0.8
35	6.9 ± 0.7	24.9 ± 0.6	8.7 ± 0.6	27 ± 0.8

Phase diagram determination: three phase line

For DPPC-d31/cholesterol, the temperature of the transition between the **so**+**lo** and **ld**+**lo** regions of the phase diagram can be determined from the midpoint of the steep decline in the first moment (M1) vs. temperature plot for a given cholesterol concentration. For PSM-d31/cholesterol, it cannot. Thus it was necessary to devise an alternative way of measuring the transition. From an examination of depaked spectra as a function of temperature, it became apparent that there was a clear change in spectral shape at the transition (Fig. S3, right column). For DPPC-d31/cholesterol this change could be pinpointed to ± 0.5 °C and agreed extremely well with the midpoint of the steep change in M1 vs. temperature. For PSM-d31/cholesterol the transition is more subtle due to the highly ordered liquid crystalline phase(s) above the transition - the spectra do not change in width very much from **so**+**lo** to **ld**+**lo**. Even so, there are

comparable changes in spectral shape between PSM-d31/cholesterol and DPPC-d31/cholesterol at the transition. For example, a peak from one of the inequivalent C2 deuterons becomes resolved (indicated by * in Fig. S3). The other major change, observed in both PSM-d31/cholesterol and DPPC-d31/cholesterol, is a sharpening of the high-frequency peak (positioned at ~55 kHz at 33 °C) at the transition. For PSM-d31/cholesterol the transition could be determined to ± 1.0 °C.
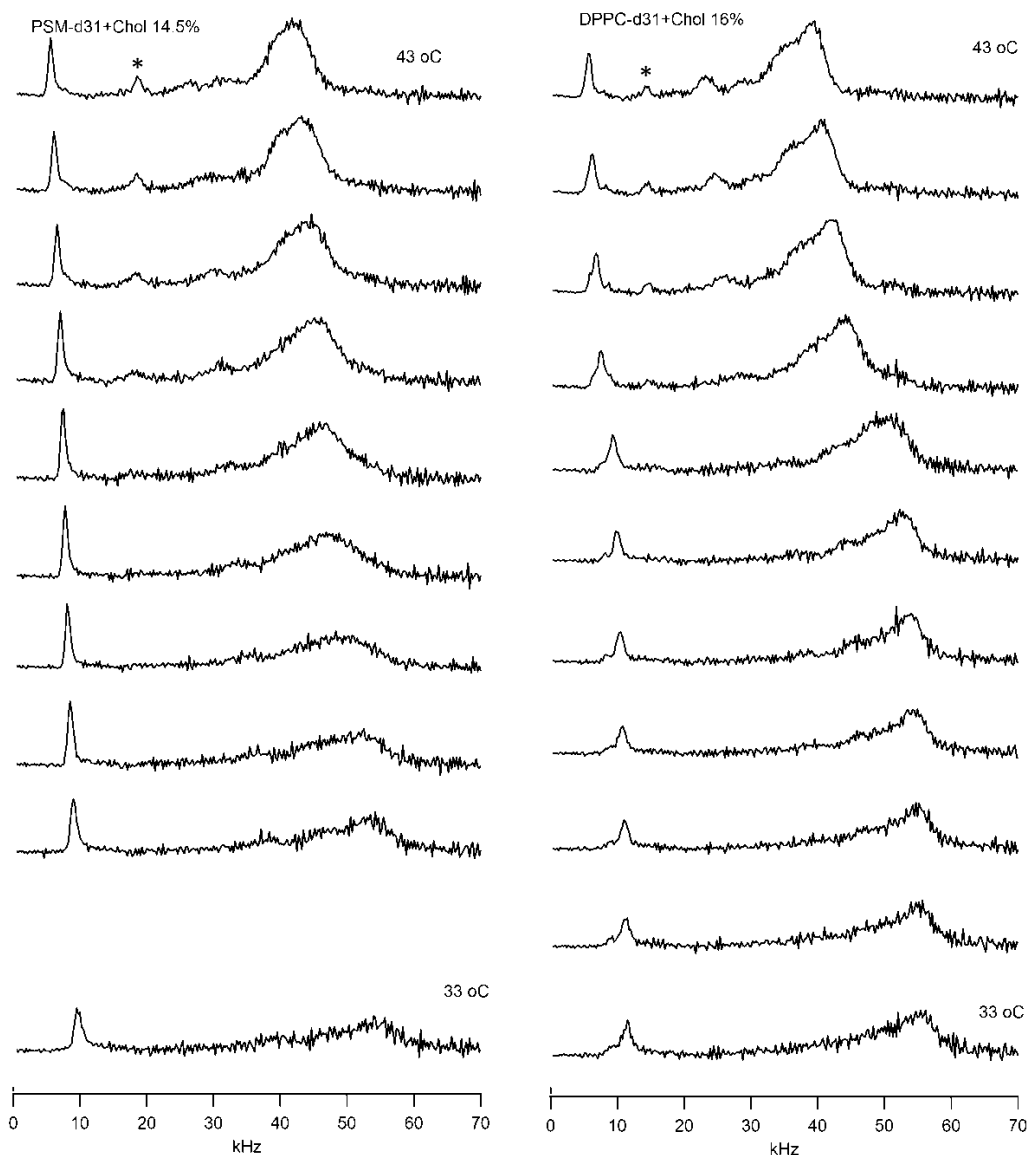

Figure S3: Determination of the temperature of the **so**+**lo** to **ld**+**lo** transition. Depaked spectra (half of each symmetric spectrum is shown) are plotted as a function of temperature at 1 degree intervals from 33 to 43 °C. Spectra of PSM-d31/cholesterol MLVs with 14.5 mol% cholesterol are shown in the left column and spectra of DPPC-d31/cholesterol MLVs with 16 mol% cholesterol are shown in the right column. The 34 °C spectrum is missing in the left column. The transition from so+lo to ld+lo occurs at 39.5 ± 0.5 °C for DPPC-d31/cholesterol, and at 38.5 ± 1.0 °C for PSM-d31/cholesterol. Asterisks indicate the resolved peak from a C2 deuteron.

Phase diagram determination, determination of the ld+lo/lo boundary:

The cholesterol concentration at the **ld+lo/lo** phase boundary can be obtained from the variation of first moment with [cholesterol] (Fig. 6). It can also be obtained from the variation of quadrupolar splitting of C12 with cholesterol concentration (Fig. S4).
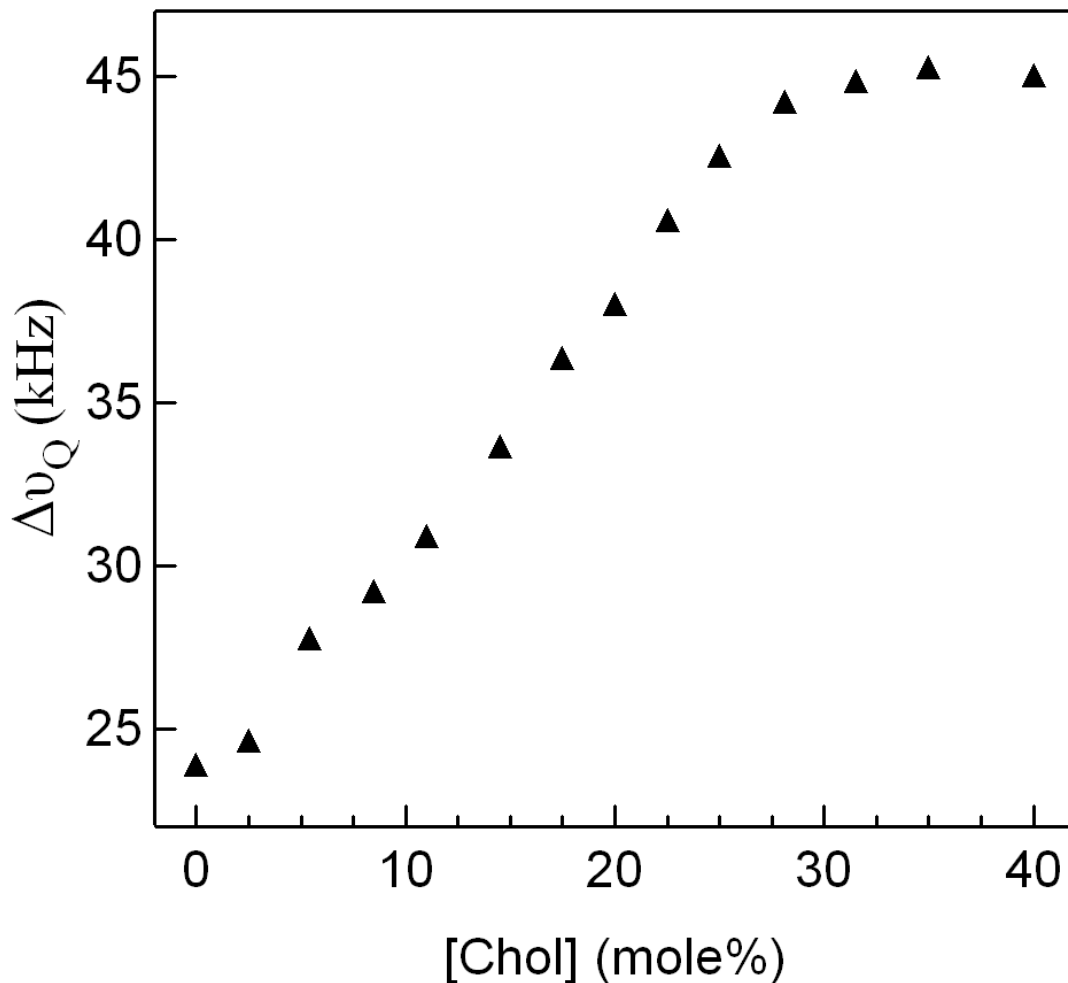

Figure S4: Quadrupolar splitting of carbon 12 on the palmitoyl chain of PSM-d31/cholesterol membranes as a function of cholesterol concentration, at T = 47°C.

SUPPLEMENTARY REFERENCE

(R1) Morrow, M. R., R. Srinivasan, and N. Grandal. 1991. The phase diagram of dimyristoyl phosphatidylcholine and chain-perdeuterated distearoyl phosphatidylcholine: A deuterium NMR spectral difference study. *Chem. Phys. Lipids*. 58:63-72.